International Journal of Pharmacognosy and Pharmaceutical Research 2025; 7(2): 158-166

International Journal of Pharmacognosy and Pharmaceutical Research

ISSN Print: 2664-7168
ISSN Online: 2664-7176
Impact Factor: RJIF 8.2
IJPPR 2025; 7(2): 158-166
www.pharmacognosyjournals.com
Received: 05-07-2025
Accepted: 10-08-2025

Isolation and identification of anti *Echis ocellatus* venom agent from *Catunaregam nilotica* (STAPF) root-bark extract

Ibrahim Sani, Angela Nnenna Ukwuani-Kwaja, Jibrin Naka Keta, Aliyu Idris Kankara, Fatima Bello, Habiba Joy Hassan Fakai, Hashimu Muhammad and Muhammad Shafi'u Abdulrauf

DOI: https://www.doi.org/10.33545/26647168.2025.v7.i2b.132

Abstract
Snakebite envenomation remains a significant cause of morbidity and mortality in tropical and subtropical regions, with conventional antivenom therapy facing limitations such as cost, hypersensitivity reactions, and limited effectiveness against local tissue damage. This study aimed to isolate and characterize a bioactive antivenom compound from the root-bark extract of *Catunaregam nilotica*, a medicinal plant widely used in African ethnomedicine for the treatment of snakebite. Dried root-bark of *Catunaregam nilotica* was extracted using absolute methanol and fractionated via successive solvent partitioning into n-hexane, ethyl acetate, and butanol fractions. The n-hexane fraction, which exhibited the highest inhibitory activity against phospholipase A_2 (PLA_2) activity was subjected to column chromatography to yield column chromatographic fractions (CPFs). These were screened *in vitro* for their inhibitory activity against snake venom metalloproteinases (SVMPs) and PLA_2 enzymes. The most potent chromatographic pooled fraction was characterized by gas chromatography-mass spectrometry (GC-MS), Fourier-transform infrared spectroscopy (FTIR), and UV-Visible (UV-Vis) spectroscopy techniques. Among the CPF18-b demonstrated the most potent inhibitory activity, significantly (p<0.05) reduced SVMP and PLA_2 activity to (1.53±0.20) and (2.99±0.08, respectively. GC-MS analysis of CPF18-b revealed a predominant single peak corresponding to P-Menth-1-en-8-ol as the possible monoterpenoid compound. FTIR spectra exhibited prominent absorption bands indicating hydroxyl (-OH) stretching at ~3372 cm^{-1} and C=C stretching at ~1630 cm^{-1} while UV-Vis spectral analysis showed a characteristic absorption maximum at 210.5 nm supporting the presence of an unsaturated alcohol functional group which is consistent with a conjugated P-Menth-1-en-8-ol structure. This study provides the first evidence of linking p-Menth-1-en-8-ol to the antivenom efficacy of *Catunaregam nilotica*, thereby supporting its traditional use in the treatment of snakebite.

Keywords: *Catunaregam nilotica*, chromatography, *echis ocellatus*, venom, enzyme inhibition, p-menth-1-en-8-ol

1. Introduction
Snakebite envenomation continues to be a critically under-recognized public health challenge in many low- and middle-income countries, particularly within sub-Saharan Africa. The World Health Organization (WHO) classifies snakebite envenoming as a neglected tropical disease (NTD) due to its significant morbidity, mortality, and socioeconomic burden, especially among rural farming populations with limited access to healthcare (WHO, 2023) [23]. Each year, an estimated 5.4 million snakebites occur globally, resulting in 1.8 to 2.7 million cases of envenomation and approximately 81,000 to 138,000 deaths (Bolon *et al.*, 2020) [35]. In Northern Nigeria, *Echis ocellatus*, commonly known as the West African saw-scaled viper, is the most medically important venomous snake, accounting for over 80-90% of reported snakebite envenomation cases in the region (Habib *et al*., 2020) [13]. The venom of *E. ocellatus* contains a complex mixture of toxic proteins, including snake venom metalloproteinases (SVMPs), phospholipase A_2 (PLA_2), serine proteases, and other procoagulant and hemorrhagic factors, which lead to extensive local tissue damage, systemic

Ibrahim Sani
Department of Biochemistry, Faculty of Life Sciences, Abdullahi Fodio University of Science and Technology, Aliero, Kebbi State, Nigeria

Angela Nnenna Ukwuani-Kwaja
Department of Biochemistry, Faculty of Life Sciences, Abdullahi Fodio University of Science and Technology, Aliero, Kebbi State, Nigeria

Jibrin Naka Keta
Department of Plant Science and Biotechnology, Faculty of Life Sciences, Abdullahi Fodio University of Science and Technology, Aliero, Kebbi State, Nigeria

Aliyu Idris Kankara
[1] Department of Biochemistry, Faculty of Life Sciences, Abdullahi Fodio University of Science and Technology, Aliero, Kebbi State, Nigeria
[2] Department of Science Laboratory Technology, Federal Polytechnic Kaura Namoda, Zamfara State, Nigeria

Fatima Bello
Department of Biochemistry, Faculty of Life Sciences, Abdullahi Fodio University of Science and Technology, Aliero, Kebbi State, Nigeria

Habiba Joy Hassan Fakai
Department of Biochemistry, Faculty of Life Sciences, Abdullahi Fodio University of Science and Technology, Aliero, Kebbi State, Nigeria

Hashimu Muhammad
[1] Department of Biochemistry, Faculty of Life Sciences, Abdullahi Fodio University of Science and Technology, Aliero, Kebbi State, Nigeria
[2] Department of Applied Science, Abdu Gusau Polytechnic, Talata Mafara, Zamfara Sate, Nigeria

Muhammad Shafi'u Abdulrauf
[1] Department of Biochemistry, Faculty of Life Sciences, Abdullahi Fodio University of Science and Technology, Aliero, Kebbi State, Nigeria
[2] Department of Biochemistry and Molecular Biology, Federal University Birnin Kebbi, Kebbi State, Nigeria

Corresponding Author:
Aliyu Idris Kankara
[1] Department of Biochemistry, Faculty of Life Sciences, Abdullahi Fodio University of Science and Technology, Aliero, Kebbi State, Nigeria
[2] Department of Science Laboratory Technology, Federal Polytechnic Kaura Namoda, Zamfara State, Nigeria

hemorrhage, and, in severe cases, multiorgan failure (Gutiérrez *et al*., 2017) [12]. The commercial antivenoms (ASVs) derived from hyperimmunized animal plasma remain the primary treatment option, their application is often hindered by several limitations. These include poor neutralization of local tissue-damaging effects, potential for serious hypersensitivity reactions, high production and procurement costs, and cold-chain storage requirements factors that collectively reduce their accessibility and effectiveness in rural and resource-poor settings (Adrião *et al*., 2022) [1]. Furthermore, current ASVs are often species-specific, which limits their utility in regions where snake identification may be difficult or multiple venomous species coexist (Resiere *et al*., 2020) [23]. As a result, there is growing interest in the identification of bioactive compounds from medicinal plants that may serve as safer, cost-effective, and more accessible alternatives or adjuncts to conventional antivenom therapy. Natural products of plant origin, particularly secondary metabolites such as flavonoids, terpenoids, tannins, and alkaloids, have shown promising enzyme inhibitory, anti-inflammatory, and tissue-protective effects in various models of snakebite envenomation (Alam and Gomes, 2003) [3].

Catunaregam nilotica (family Rubiaceae), a shrub native to tropical Africa, is traditionally used in Northern parts of Nigeria for the treatment of venomous bites (Sani *et al*., 2024) [25]. Although ethnobotanical reports support its use in snakebite treatment, the specific phytoconstituents responsible for this activity remain largely uncharacterized. Recent preliminary screenings suggest the presence of bioactive compounds with enzyme inhibitory activity (Hassan *et al*., 2023) [14], but detailed isolation and structural elucidation are lacking. Therefore, the present study aimed to isolate and identify the key bioactive compound from the root-bark of *Catunaregam nilotica* using a bioactivity-guided fractionation approach.

2. Materials and Methods

2.1 Collection and Authentication of Plant Material

Fresh root-bark of *Catunaregam nilotica* was collected from Kaura Namoda, Zamfara State, Northwestern Nigeria, during the dry season (November-January). The plant material was identified and authenticated by Professor Dramendra Singh. A voucher specimen (KSUSTA/PSB/H/Voucher No. 234A) was deposited at the Herbarium, Department of Plant Science and Biotechnology, Kebbi State University of Science and Technology, Aliero (KSUSTA).

2.2 Venom Source and Preparation

Lyophilized *Echis ocellatus* venom was bought in March, 2024 from the pharmacology department at Ahmadu Bello University Zaria. And was reconstituted in phosphate-buffered saline (PBS, pH 7.4) and stored in aliquots at 20 ^{0}C. Working dilutions were freshly prepared before each experimental procedure.

2.3 Extraction and Fractionation of *Catunaregam nilotica* Root-bark and Preliminary Assessment of PLA_2 Inhibition

The extraction, solvent fractionation, and *in vitro* enzyme inhibition assay were performed following procedures previously described in detail by ((Idris *et al*., 2024) [16]. In that study, the crude methanol extract and solvent fractions of *Catunaregam nilotica* root-bark were evaluated for their inhibitory effects on PLA_2 activity of *Echis ocellatus* venom.

2.4 Column Chromatography of the n-Hexane Fraction

The n-hexane fraction, which demonstrated the highest inhibitory activity in preliminary enzyme assays, was subjected to open-column chromatography on silica gel (60-120 mesh). Ten grams of the fraction were loaded onto the column and eluted with a stepwise gradient of n-hexane and ethyl acetate (100:0 to 0:100, v/v). Eluates were collected in 20 mL portions and monitored using thin-layer chromatography (TLC) on silica gel plates (Jimoh *et al*., 2021) [17].

2.5 Thin-Layer Chromatography (TLC)

TLC was performed using n-hexane:ethyl acetate (65:35, v/v) as the mobile phase. Plates were developed by capillary action and air-dried. Spots were visualized by spraying with vanillin reagent (1 g vanillin in 94 mL ethanol and 5 mL concentrated H_2SO_4) and heating at 100 °C for 3-7 min (Sani *et al*., 2020 Ahmed et a., 2022) [26, 2]. Fractions showing similar TLC profiles were combined to yield 18 chromatographic pooled fractions (CPF1-CPF18), which were concentrated to dryness and evaluated for *in vitro* enzyme inhibitory activity.

2.6. *In vitro* Enzyme Inhibition Assays

2.6.1. Snake Venom Metalloproteinase (SVMP) Inhibition Assay

SVMP inhibition was assessed following the method of Greenberg *et al*. (1955) [11] with slight modifications. The reaction mixture contained 0.5% (w/v) casein, 1.0 mL of Tris-HCl buffer (pH 8.0), and 0.5 mL of *Echis ocellatus* venom (0.25% w/v). The mixture was incubated at 37 °C for 4 h, and the reaction was terminated by adding trichloroacetic acid (TCA). The filtrate was collected, and 1.0 mL was analyzed for protein content using the Lowry method (Lowry *et al*., 1951) [19], with L-tyrosine as the standard. For inhibition studies, *E. ocellatus* venom (0.25% w/v) was pre-incubated with either the column chromatographic fraction (CPF) of *Catunaregam nilotica* (0.1 mg/mL) root-bark methanol extract at 37 °C for 30 min prior to addition to the reaction mixture. A venom-only control was included. Enzyme activity was calculated as follow:

$$\text{Enzyme activity} = \frac{\mu mol\ of\ tyrosine\ released}{Time\ taken\ in\ minutes}$$

Protein concentration was determined as:

$$\text{Protein concentration} = \frac{Absorbance\ of\ test}{Absorbance\ of\ control} \times Conc\ of\ STD$$

Relative enzyme activity and inhibition were expressed as:

$$\%\ \text{Activity} = \frac{Enzyme\ activity\ of\ the\ test}{Enzyme\ activity\ of\ the\ control} \times 100$$

2.6.2 Phospholipase A_2 (PLA_2) Inhibition Assay

Phospholipase A_2 inhibition was evaluated using the acidimetric method of Tan and Tan (1988) [27] with minor modifications. A substrate mixture containing 18 mM $CaCl_2$, 1% (v/v) Tween-80, and 2 mg/mL egg yolk was homogenized and adjusted to pH 8.0 using 1 M NaOH and 1 N HCl. The reaction was initiated by adding *E. ocellatus* venom (0.1 mg/mL) to 15 mL of the substrate mixture, while saline served as the negative control. For inhibition studies, venom (0.1 mg/mL) was pre-incubated with either CPF or CPF18 (0.1 mg/mL) at 37 °C for 30 min before addition to the substrate. The decrease in pH was monitored every 2 min using a calibrated pH meter. A one-unit decrease in pH corresponded to the release of 133 µmol of fatty acids (Yap *et al*., 2011) [32].

$$\text{Enzyme activity} = \frac{\mu mol\ of\ FA\ released}{Time\ taken\ in\ minutes}$$

$$\%\ \text{Activity} = \frac{Enzyme\ activity\ of\ the\ test}{Enzyme\ activity\ of\ the\ control} \times 100$$

Percentage inhibition % =100- enzyme activity (Hassan *et al*., 2023) [14]

Where: FA = Fatty acid

2.7 Spectroscopic Characterization of Chromatographic Pooled Fraction-18 (CPF18)

2.7.1 GC-MS analysis

GC-MS analysis of the CPF18 obtained from the *n*-hexane fraction of *Catunaregam nilotica* root-bark was performed using a Shimadzu GCMS-QP2010 Plus system equipped with an AOC-20i auto-injector and HP-5MS fused silica capillary column (30 m × 0.25 mm i.d., 0.25 µm film thickness) (Tarik, et al., 2024) [28]. Approximately 2 mg of the dried CPF18 was dissolved in 1 mL analytical-grade *n*-hexane, vortexed, sonicated for 10 min, and filtered through a 0.22 µm PTFE syringe filter. Helium served as the carrier gas at 1.0 mL/min. The injector temperature was 250 °C, and 1 µL of the sample was injected in split mode (10:1). The oven temperature was programmed from 60 °C (2 min hold) to 280 °C at 10 °C/min with a final hold of 10 min. Mass spectra were obtained under electron impact ionization (70 eV), with ion source and quadrupole temperatures of 230 °C and 150 °C, respectively. Data were collected in full-scan mode (m/z 50-650). Compounds were identified by comparing their spectra with those in the NIST and Wiley libraries (Corporation Shimadzu, 2010) [7].

2.7.2 Fourier Transform Infrared (FT-IR) Spectroscopic Analysis

FT-IR analysis was carried out to identify the functional groups present in the CPF18. The sample was homogenized with KBr (1:19 w/w) and pressed into a transparent pellet using a hydraulic press. Spectra were recorded over the range 400-4000 cm^{-1} at a resolution of 4 cm^{-1} using a Thermo Nicolet AVATAR 330 spectrometer. The absorption peaks were interpreted to identify characteristic vibrational modes corresponding to major functional groups (Devi and Battu, 2019; Shimadzu, 2014) [8, 7].

2.7.3 Ultraviolet-Visible (UV-Vis) Spectroscopic Analysis

UV-Vis spectroscopy was employed to determine electronic transitions and chromophoric characteristics of the CPF18. About 1 mg of the dried sample was dissolved in 10 mL methanol and filtered through a 0.22 µm PTFE syringe filter. The absorption spectrum was recorded in the wavelength range 200-800 nm using a Shimadzu UV-1800 double-beam spectrophotometer with methanol as blank. The absorption maxima (λmax) were analyzed to infer the presence of conjugated and aromatic systems indicative of bioactive compounds (Thermo Fisher Scientific, 2003) [29].

2.8 Statistical Analysis

All enzyme inhibition assays were performed in triplicate. Results were expressed as mean±standard deviation (SD). Statistical comparisons between groups were carried out using one-way ANOVA followed by Tukey's post hoc test. Significance was set at $p<0.05$. Data analysis was performed using SPSS 20 Version.

3. Results

3.1 Differential Inhibitory Effects of *Catunaregam nilotica* Root-Bark Fractions on the Enzymatic Activities of *Echis ocellatus* Venom.

The present investigation builds upon our earlier findings (Idris *et al*., 2024) [16], which demonstrated the potent inhibitory effects of *Catunaregam nilotica* root-bark fractions against the enzymatic activities of *E. ocellatus* venom. In that study, the n-hexane fraction exhibited the highest inhibitory potency, particularly against phospholipase A_2 (PLA_2) and snake venom metalloproteinases (SVMPs), while the ethyl acetate fraction showed moderate inhibition and the aqueous and n-butanol fractions exhibited comparatively weaker effects.

3.2 Column Chromatographic Separation of the *n*-Hexane Fraction of *Catunaregam nilotica* Root-bark Methanol Extract

The *n*-hexane fraction of *Catunaregam nilotica* root-bark methanol extract was subjected to open-column chromatography, yielding a total of 140 fractions (20 mL each). Based on similarities in TLC mobility profiles, these fractions were pooled into 18 chromatographic pooled fractions (CPFs), designated CPF1-CPF18 (Table 3.1). The color of the fractions ranged from colorless to various shades of yellow, brown, and black, indicating compositional diversity among fractions. TLC analysis revealed distinct retention factor (Rf) values (0.33-0.82) and varying numbers of spots (1-3 per CPF).

Table 3.1 Column Chromatographic Separation of the *n*-Hexane Fraction of *Catunaregam nilotica* Root-bark Methanol Extract

CPF Code	Fractions Pooled	No. of TLC Spots	Rf Values	Color
CPF1	F1-F4	2	0.80, 0.72	Pale yellow
CPF2	F5-F10	3	0.76, 0.63, 0.40	Colorless
CPF3	F11-F15	2	0.69, 0.52	Yellow
CPF4	F16-F20	2	0.82, 0.75	Dark yellow
CPF5	F21-F35	3	0.65, 0.48, 0.34	Yellow
CPF6	F36-F40	1	0.60	Pale brown
CPF7	F41-F42	2	0.71, 0.59	Light brown
CPF8	F43-F50	2	0.67, 0.50	Yellow
CPF9	F51-F61	1	0.74	Dark yellow
CPF10	F62-F70	3	0.69, 0.55, 0.42	Yellow
CPF11	F71-F75	2	0.60, 0.48	Light brown
CPF12	F76-F85	2	0.71, 0.33	Brown
CPF13	F86-F101	3	0.66, 0.50, 0.37	Yellow
CPF14	F102-F105	2	0.72, 0.61	Brown
CPF15	F106-F110	2	0.70, 0.54	Brown
CPF16	F111-F115	1	0.68	Brown
CPF17	F116-F130	2	0.62, 0.45	Yellow
CPF18	F131-F140	2	0.74, 0.60	Light brown

3.3 *In vitro* Antivenom Potential of Chromatographic Pooled Fractions (CPFs) of n-Hexane Fraction of *Catunaregam nilotica* Root-bark Methanol Extract

3.3.1 Inhibition of Snake Venom Metalloproteinase (SVMP) Activity

The *in vitro* inhibition of *Echis ocellatus* SVMP activity by CPFs is shown in Figure 3.1. SVMP activity varied from 0.92 to 8.81 U/L among the fractions. The venom control group exhibited the highest activity (13.75 U/L) with no inhibition, while antivenom (ASV) treatment achieved 90.8% inhibition, reducing activity to 1.26 U/L. Among the test fractions, CPF18 exhibited the most potent inhibitory effect, reducing SVMP activity by 90.1%, comparable ($p>0.05$) to ASV. Similarly, CPF4, CPF7, CPF8, and CPF10 also demonstrated strong inhibition, showing no significant difference ($p>0.05$) from ASV.

3.3.2 Inhibition of Phospholipase A_2 (PLA_2) Activity

As shown in Figure 3.2, the inhibitory effects of CPFs on *Echis ocellatus* PLA2 activity varied significantly ($p<0.05$). The venom control group exhibited the highest PLA2 activity (8.47±0.00 U/L), while ASV achieved a 90.6% inhibition (0.79±0.03 U/L). Among the fractions, CPF18 displayed the strongest inhibition (72.4%), followed by CPF15 (64.7%) and CPF14 (63.7%), whereas CPF3 showed the weakest inhibition (7.5%). These results confirm CPF18 as the most bioactive chromatographic fraction against PLA_2.

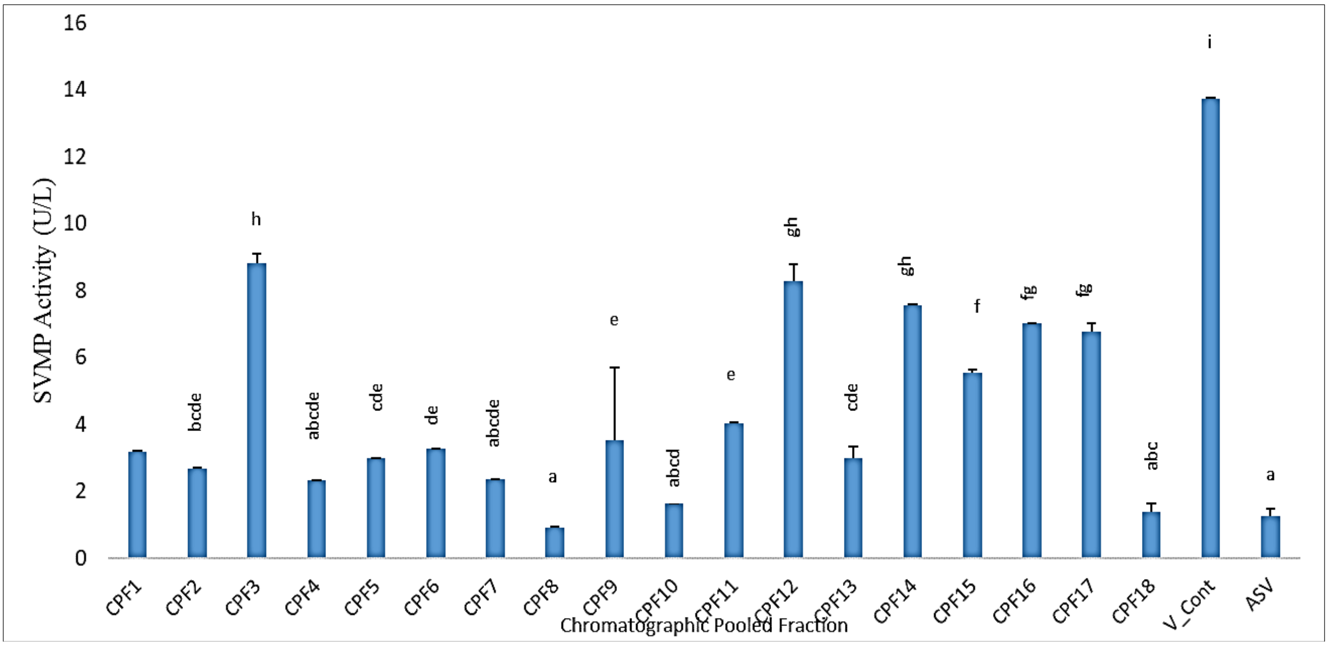

Fig 3.1: *In vitro* inhibition of SVMP activity of Echis ocellatus venom by chromatographic pooled fraction of Catunaregam nilotica. Mean enzyme activity carrying different superscripts were significantly ($P<0.05$) different, (n=3)

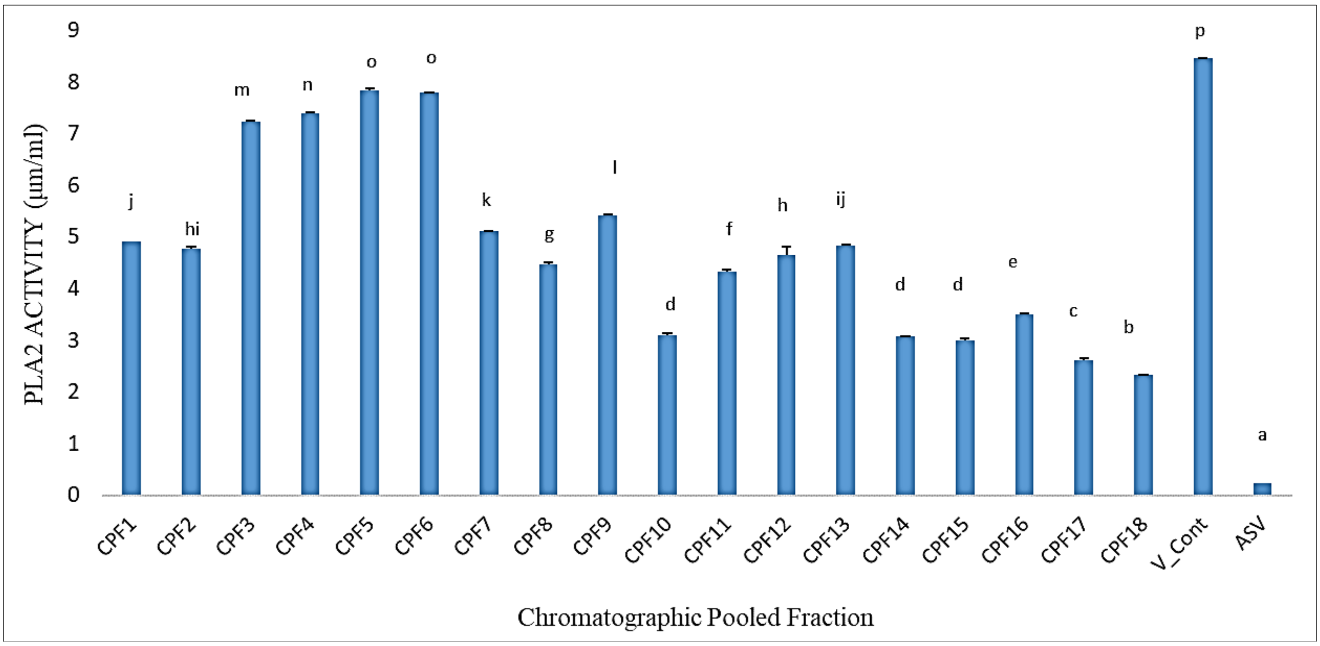

Fig 3.2: *In vitro* inhibition of PLA_2 activity of Echis ocellatus venom by chromatographic pooled fraction of Catunaregam nilotica root-bark n-hexane fraction. Mean enzyme activity carrying different superscripts were significantly ($P<0.05$) different, (n=3)

3.4 TLC Profiling of Bioactive Components of *n*-Hexane Fraction of *Catunaregam nilotica* Root-Bark Extract and Chromatographic Pooled Fraction-18

TLC analysis of the CPF18 alongside the parent *n*-hexane fraction revealed two distinct spots (Plate 3.3), indicating the presence of two phytochemically distinct components, provisionally designated CPF18-a and CPF18-b.

3.5. *In vitro* Inhibition of SVMP Activity by CPF18-a and CPF18-b

As shown in Figure 3.3, both subfractions inhibited SVMP activity, with CPF18-b demonstrating superior efficacy. CPF18-b reduced SVMP activity to 1.53±0.20 U/L (88.9% inhibition), whereas CPF18-a achieved a moderate inhibition of 69.5%. The venom control recorded 13.75±0.03 U/L activity (0% inhibition), while ASV achieved 91.5% inhibition (1.17±0.01 U/L). These findings indicate that CPF18-b possesses strong SVMP-neutralizing potential comparable to ASV.

3.6. *In vitro* Inhibition of PLA_2 Activity by CPF18-a and CPF18-b

Figure 3.4 depicts the inhibitory effects of CPF18 subfractions on PLA_2 activity. CPF18-b exhibited the greatest inhibition (67.1%), reducing PLA_2 activity to 2.79±0.08 U/L, while CPF18-a showed 39.9% inhibition (5.09±0.49 U/L). The venom control group maintained the highest activity (8.47±0.00 U/L), whereas ASV achieved the highest inhibition (90.7%, 0.79±0.04 U/L). These results affirm the potent dual enzyme inhibitory capacity of CPF18-b.

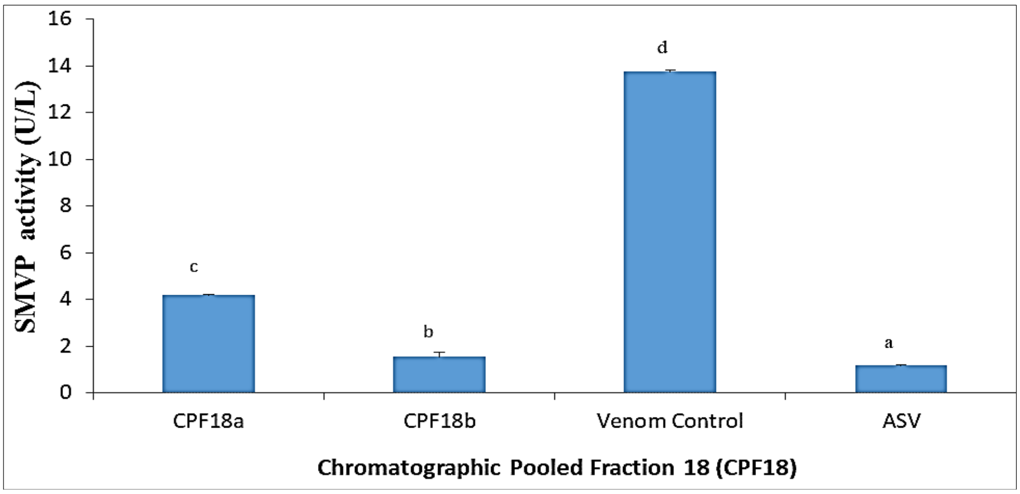

Fig 3.3: *In vitro* inhibition of SVMP activity of Echis ocellatus venom by CPF18-a, and CPF18-b of Catunaregam nilotica. Mean enzyme activity carrying different superscripts are significantly (P<0.05) different using ANOVA and Duncan multiple comparison test, (n=3).

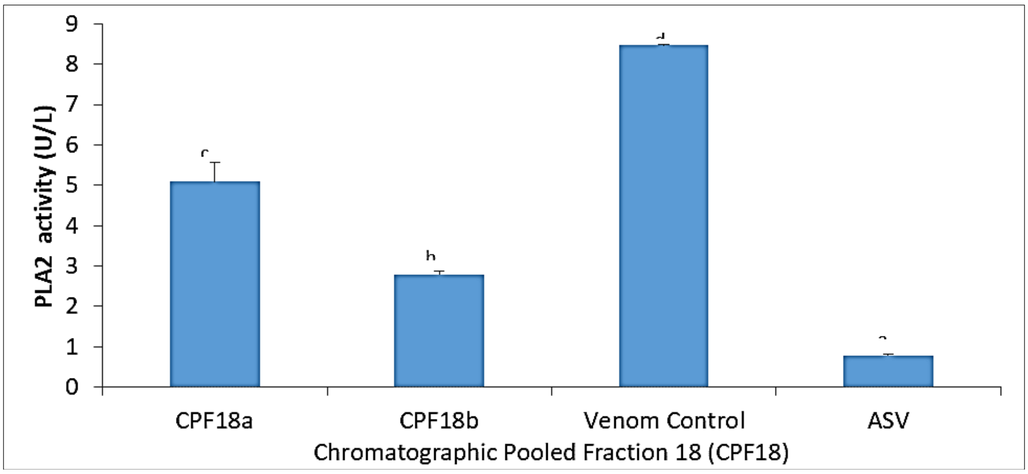

Fig 3.s4: *In vitro* inhibition of PLA_2 activity of *Echis ocellatus* venom by CPF18-a, and CPF18-b of *Catunaregam nilotica*. Mean enzyme activity carrying different superscripts is significantly (P<0.05) different using ANOVA and Duncan multiple comparison test, (n=3)

3.7 TLC Profiling of Bioactive Component CPF18-b

TLC profiling of CPF18-b (Plate 3.4) displayed a single distinct spot (Rf = 0.88), confirming it as a single compound.

3.8 Spectroscopic Characterization of the Bioactive Compound (CPF18-b)

3.8.1 GC-MS Analysis

GC-MS analysis of CPF18-b (Table 3.3; Figure 3.5) identified a single major compound, *p*-Menth-1-en-8-ol (Terpinol) as the possible compound, with a retention time (RT) of 23.740 min. The compound exhibited a molecular formula of $C_{10}H_{18}O$ and a molecular weight of 154 g/mol, representing 100% of the chromatographic peak area, classifying it as a monoterpenoid alcohol.

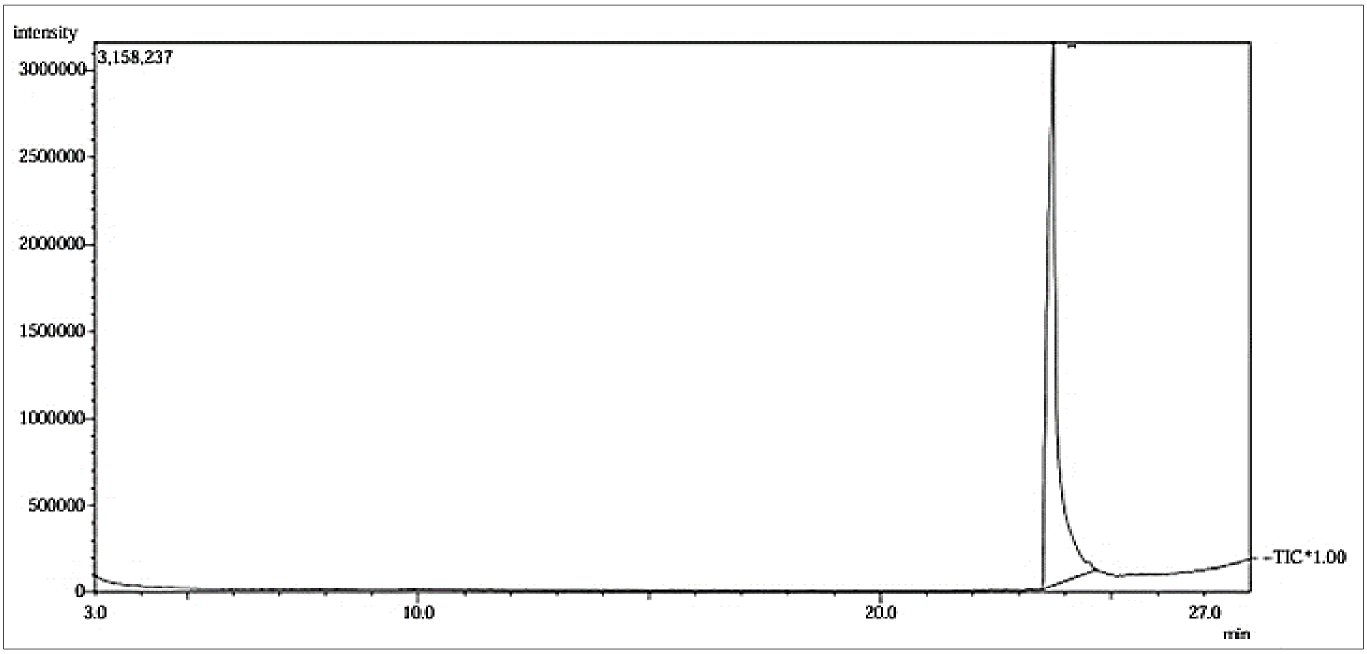

Fig 3.5: GC-MS chromatogram of CPF18-b isolated from *Catunaregam nilotica* root-bark n-hexane fraction

Table 3.3: GC-MS Analysis of CPF18-b of n-Hexane Fraction of Crude Methanol Extract of Catunaregam nilotica Root-bark

Peak	Retention Time (RT)	Compound Name	Molecular Formula	Molecular Structure	Molecular Weight (g/mol)	% Peak Area	Class of Compound
1	23.740 min	P-Menth-1-en-8-ol (Terpinol)	$C_{10}H_{18}O_3$	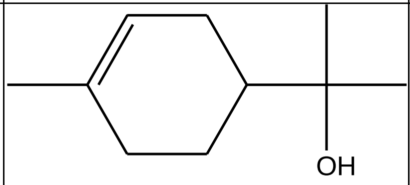 P-Menth-1-en-8-ol	154	100	**Terpenoid alcohol**

3.8.2 FT-IR Spectroscopy

The FT-IR spectrum (Table 3.4; Figure 3.6) of CPF18-b revealed key functional group vibrations: O-H stretching (3356.25 cm^{-1}), C=C stretching (1643.41 cm^{-1}) confirming the presence of alcohol and alkene functionalities consistent with Terpinol. And weak peaks at 2137.20 cm^{-1} (C≡C or C≡N stretching) due to impurities or secondary interactions.

Table 3.4: FTIR Spectral Data of CPF18-b Isolated from *Catunaregam nilotica* Root-Bark n-Hexane Fraction.

Wavenumber (CM^{-1})	Intensity	Assignment	Interpretation
1643.41	77.507	C=C stretching (alkene)	Confirms the presence of a double bond
3356.25	58.616	O-H stretching (alcohol)	Confirms the hydroxyl functional group
2137.2	97.757	C≡C (alkyne) or C≡N (nitrile) stretching	Likely due to a minor impurity or secondary interaction
3765.17	95.567	Free O-H stretching	Supports the presence of an alcohol group

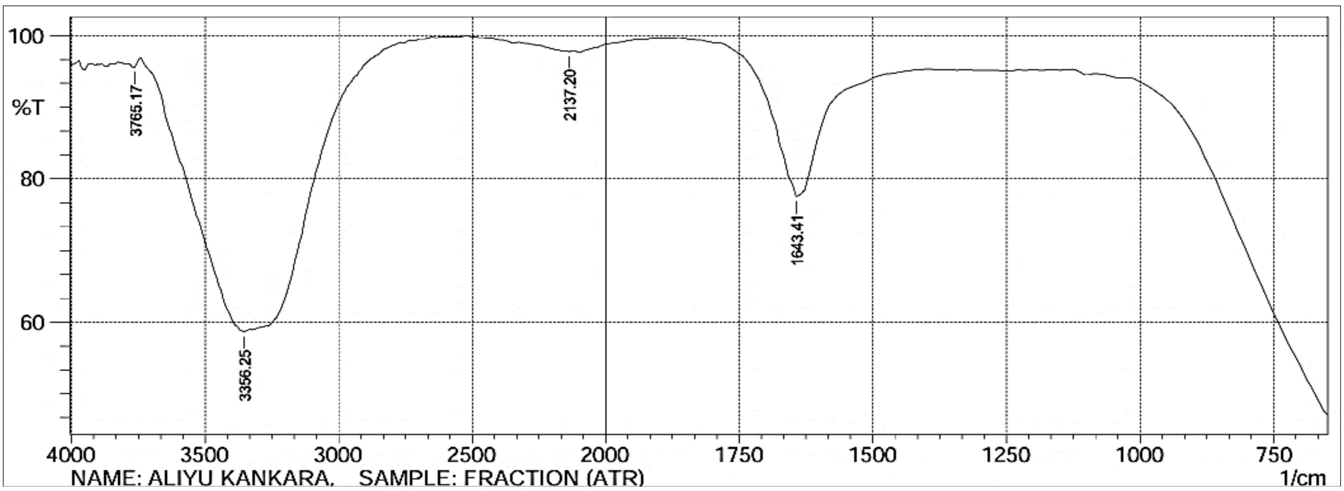

Fig 3.6: FTIR spectral of CPF18-b Isolated from Catunaregam nilotica Root-Bark n-Hexane Fraction

3.8.3 UV-Visible Spectroscopy

UV-Vis spectroscopic analysis (Table 3.5; Figure 3.7) displayed a strong absorption peak at 210.50 nm (A = 2.580), indicative of π→π* or n→π* transitions associated with conjugated C=C and C=O systems, and a minor band at 215.00 nm (A = 0.078).

Table 3.5: UV Spectral Data of CPF18-b Isolated from *Catunaregam nilotica* Root-Bark n-Hexane Fraction

Wavelength (nm)	Absorbance	Possible Transition	Interpretation
210.50	2.580	π→π* or n→π*	Conjugated C=C and C=O system
215.00	0.078	Minor transition	Secondary chromophore or an impurity

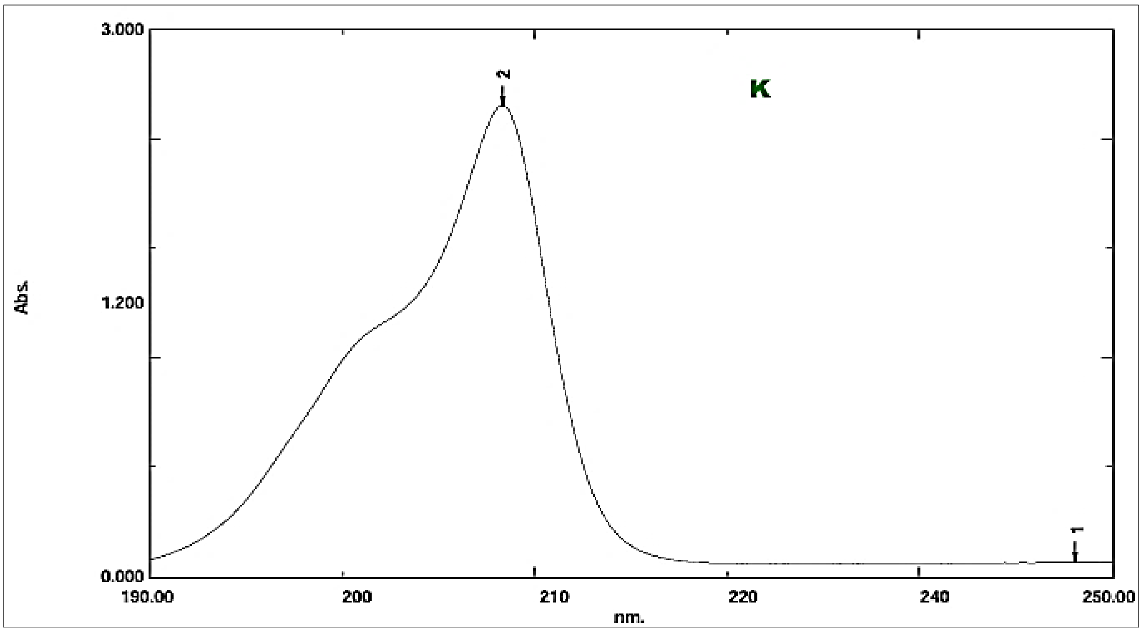

Fig 3.7: UV-Vis spectrum of CPF18-b Isolated from *Catunaregam nilotica* Root-bark n-hexane fraction

4. Discussion

Chromatographic separation of the *n*-hexane fraction (n-HF) of *Catunaregam nilotica* produced 18 pooled fractions, among which CPF18b exhibited the strongest inhibitory activity against SVMP and PLA_2 enzymes of *Echis ocellatus* venom. This fraction, designated as the Chromatographic Pooled Fraction-18 (CPF18-b), likely owes its bioactivity to specific phytochemicals capable of neutralizing venom enzymes through direct binding, metal ion chelation, or antioxidant mechanisms. SVMPs are zinc-dependent endopeptidases primarily responsible for local hemorrhage, degradation of basement membranes, and tissue necrosis (Gutiérrez *et al*., 2017) [12]. Inhibition of SVMPs by CPF18-b suggests that this compound interferes with proteolytic cleavage, likely through direct binding or chelation of catalytic metal ions, a mechanism proposed for phytochemicals (Alam and Gomes, 2003; Samy *et al*., 2021) [3, 24]. Similarly, PLA2 enzymes catalyze the hydrolysis of phospholipids in cell membranes, leading to inflammation, myotoxicity, and disruption of cellular integrity (Castro-Amorim *et al*., 2023) [6]. The significant PLA_2 inhibition observed in this study aligns with previous reports of plant-derived secondary metabolites attenuating venom toxicity by targeting this enzymatic pathway (Xiao *et al*., 2017) [31]. The dual inhibition of SVMP and PLA_2 highlights the broad-spectrum potential of CPF18-b against snake venom-induced pathophysiology. These findings corroborate earlier reports identifying flavonoids, alkaloids, polyphenols, and terpenoids as potent inhibitors of SVMPs and PLA_2 due to their interference with enzymatic active sites and mitigation of venom-induced oxidative stress (Yusuf *et al*., 2024; Yusuf *et al*., 2021) [34, 33]. Building upon dual inhibitory activities demonstrated by CPF-18b against SVMP and PLA_2 of *Echis ocellatus* venom, a bioactivity-guided isolation protocol was employed to isolate and characterize the active compound responsible for antivenom effects displayed by n-hexane fraction of *Catunaregam nilotica* root-bark extract.

Gas Chromatography-Mass Spectrometry (GC-MS) analysis indicated p-Menth-1-en-8-ol (Terpinol; m/z ≈ 154) as the possible compound present in the active fraction (CPF18-b), which dominated the chromatographic profile. This observation suggests that the fraction is composed primarily of a single monoterpenoid alcohol. These findings are consistent with previous reports describing comparable chromatographic and mass spectral profiles for monoterpenes (Naviglio *et al*., 2015; El-Sayed, 2024) [21, 9]. Supporting evidence from Fourier Transform Infrared (FTIR) and Ultraviolet-Visible (UV-Vis) analyses further validated the compound's structural characteristics, showing absorption bands attributable to hydroxyl and alkene functional groups typically associated with terpenoid alcohols. These spectral features closely resemble those reported for monoterpenoids in earlier studies (FTIR Functional Group Database, 2025; Casoni *et al*., 2024; Hu *et al*., 2010; [10, 5, 15] (Amarvani and Ramesh, 2020) [4]. Collectively, these results corroborate previous findings describing similar compounds in medicinal plants and essential oils, which are known for their antimicrobial, antioxidant, and anti-inflammatory activities (Khaleel *et al*., 2018; Masyita *et al*., 2022; Prerna *et al*., 2024) [18, 20, 22]. This may partly explain the observed biological activity of the fraction and its potential role in the antivenom efficacy of *Catunaregam nilotica*.

Conclusion

The findings from this study demonstrate that the n-hexane fraction of *Catunaregam nilotica* root-bark methanol extract contains bioactive constituents capable of neutralizing key enzymatic components of *Echis ocellatus* venom. Among the 18 pooled fractions obtained, CPF-18b demonstrated the most potent inhibitory effects against SVMP and PLA_2, venom enzymes responsible for most the local and systemic toxic effects of snake envenomation. Chromatographic and Spectroscopic (FT-IR and UV-visible) analyses identified p-Menth-1-en-8-ol (Terpinol) as the possible compound present in CP18-b. This study provides the first evidence linking of p-Menth-1-en-8-ol to the antivenom efficacy of *Catunaregam nilotica*, thereby supporting its traditional use in the treatment of snakebite.

References

1. Adrião A, dos Santos A, de Lima E, Maciel J, Paz W, da Silva F, *et al*. Plant-derived toxin inhibitors as potential candidates to complement antivenom treatment in snakebite envenomations. Front Immunol. 2022; 13:325-329. doi:10.3389/fimmu.2022.842576.
2. Ahmed M, Arise R, Umaru I. Identification and biochemical characterization of anti-enteropooling compounds from *Annona senegalensis* root bark. Sci Afr. 2022;15: e01128. doi: 10.1016/j.sciaf. 2022.e01128.
3. Alam MI, Gomes A. Snake venom neutralization by Indian medicinal plants (*Vitex negundo* and *Emblica officinalis*) root extracts. J Ethnopharmacol. 2003;86(1):75-80. doi:10.1016/S0378-8741(03)00049-7.
4. Amarvani PK, Ramesh L. Isolation, purification and characterization of terpene from *Ficus krishnae*. Pharmacophore. 2020;11(2):30-35.
5. Casoni D, Cobzac S, Simion I. Feasibility of UV-Vis spectroscopy combined with pattern recognition techniques to authenticate the medicinal plant material from different geographical areas. J Anal Sci Technol. 2024; 15:17. doi:10.1186/s40543-024-00428-2.
6. Castro-Amorim J, de Oliveira A, Da Silva S, Soares A, Mukherjee A, Ramos M, *et al*. Catalytically active snake venom PLA2 enzymes: an overview of its elusive mechanisms of reaction. J Med Chem. 2023;66(8):5364-5376. doi: 10.1021/acs.jmedchem.3c00097.
7. Shimadzu Corporation. GCMS-QP2010 Plus Gas Chromatograph Mass Spectrometer Instruction Manual. Japan: Shimadzu Corp.; 2010.
8. Devi D, Battu G. Qualitative phytochemical screening and FTIR spectroscopic analysis of *Grewia tilifolia* (Vahl) leaf extracts. Int J Curr Pharm Res. 2019;11(4):100-107. doi:10.22159/ijcpr.2019v11i4.34936.
9. El-Sayed AM. The pherobase: Database of pheromones and semiochemicals. 2024.
10. InstaNANO. FTIR functional group database table with search. 2025 Oct 13. Available from: https://instanano.com/all/characterization/ftir/ftir-functional-group-search
11. Greenberg D, Colowick S, Kalpan N. Plant proteolytic enzymes. In: Methods in Enzymology. New York: Academic; 1955. p.54-64.
12. Gutiérrez J, Calvete J, Habib A, Harrison R, Williams D, Warrell D. Snakebite envenoming. Nat Rev Dis Primers. 2017;3(17063):1-10. doi:10.1038/nrdp.2017.63.
13. Habib A, Musa B, Iliyasu G, Hamza M, Kuznik A, Chippaux P. Challenges and prospects of snake antivenom supply in sub-Saharan Africa. PLoS Negl Trop Dis. 2020;14(8):1-10. doi: 10.1371/journal.pntd.0008374.
14. Hassan L, Faruq U, Yusuf A, Salihu M. *In vitro* detoxifying effects of *Catunaregam nilotica* (Stapf) root extracts against *Naja nigricollis* phospholipase A2 enzyme. Nile J Eng Appl Sci. 2023;1(1):81-89. doi:10.5455/NJEAS.150317.
15. Hu S-X, Yu J-G, Zeng EY. A theoretical study on UV-spectroscopy, electronic structure and reactivity properties of sesquiterpenes. Atmos Chem Phys. 2010; 10:24325-24343. doi:10.5194/acpd-10-24325-2010.
16. Idris AK, Ibrahim A, Emmanuel O. *In vitro* anti-venom effect of *Catunaregam nilotica* (Stapf) root extracts against *Echis ocellatus* phospholipase A2 activity. Asian J Res Biochem. 2024;14(6):232-240. doi:10.9734/ajrb/2024/v14i6344.
17. Jimoh A, Ilyas M, Sani Y, Bakare L, Adejoke S. Isolation of stigmasterol from the root bark of *Annona senegalensis* Pers. (Annonaceae). Niger Res J Chem Sci. 2021;186-196.
18. Khaleel C, Tabanca N, Buchbauer G. α-Terpineol, a natural monoterpene: a review of its biological properties. Open Chem. 2018;16(1):349-361. doi:10.1515/chem-2018-0040.
19. Lowry O, Rosebrough N, Farr A, Randall R. Protein measurement with the Folin phenol reagent. J Biol Chem. 1951;193(1):265-275.
20. Masyita A, Mustika SR, Dwi Astuti A, Yasir B, Rahma Rumata N, Emran T, *et al*. Terpenes and terpenoids as main bioactive compounds of essential oils. Food Chem X. 2022; 13:100217. doi: 10.1016/j.fochx.2022.100217.
21. Naviglio D, Le Grottaglie L, Vitulano M, Trifuoggi M, Gallo M. Characterization of essential oil components from aromatic plants in “Piana del Sele”, Italy, using GC-MS. Nat Prod Commun. 2015;10(7):1293-1296.
22. Prerna P, Chadha J, Khullar L, Mudgil U, Harjai KA. Comprehensive review on the pharmacological prospects of terpinen-4-ol. Fitoterapia. 2024;106051. doi: 10.1016/j.fitote.2024.106051.
23. Resiere D, Monteiro W, Houcke S, Pujo J, Mathien C, Mayence C. *Bothrops* snakebite envenomings in the Amazon region. Curr Trop Med Rep. 2020; 7:48-60. doi:10.1007/s40475-020-00203-4.
24. Samy PR, Gopalakrishnakone P, Chow V. Therapeutic application of natural inhibitors against snake venom phospholipase A2. Bioinformation. 2012;8(1):48-57. doi:10.6026/97320630008048.
25. Sani I, Ukwuani-Kwaja A, Zubairu A, Fakai M, Bello F, Sani H. Antivenom potentials of some local medicinal plants against *Naja nigricollis* envenoming in Nigeria. Pharmacologia. 2024;15(1):15-22. doi:10.17311/pharmacologia.2024.15.22.
26. Sani I, Umar R, Hassan S, Faruq U, Bello F, Abdulhamid A. Inhibition of snake venom enzymes and antivenom adjuvant effects of *Azadirachta indica* A. Juss. leaf extracts. Eur J Med Plants. 2020;31(10):114-128. doi:10.9734/EJMP/2020/v31i1030288.

27. Tan N, Tan C. Acidimetric assay for phospholipase A2 using egg yolk suspension. Anal Biochem. 1988;170(2):282-288.
28. Tarik R, Drioiche A, El Amri J, Ed-Dahmouny M, Shahat AA, Hadi N, *et al*. Phytochemical profiling and bioactivity assessment of *Teucrium capitatum* L. essential oil and extracts. Pharmaceuticals. 2024;17(12):1578. doi:10.3390/ph17121578.
29. Thermo Fisher Scientific Inc. User Guide: Nicolet Avatar 330 FT-IR Spectrometer. Madison, USA: Thermo Electron Corp.; 2003.
30. World Health Organization. Snakebite envenoming: key facts. 2023. Available from: https://www.who.int/news-room/fact-sheets/detail/snakebite-envenoming
31. Xiao H, Pan H, Liao K, Yang M, Huang C. Snake venom PLA2, a promising target for antivenom drug development. 2017;6592820. doi:10.1155/2017/6592820.
32. Yap M, Tan N, Fung S. Biochemical and toxinological characterization of *Naja sumatrana* venom. J Venom Anim Toxins Trop Dis. 2011;17(4):451-459.
33. Yusuf A, Aleko G, Bello R, Liman D. Prospects and challenges of developing plant-derived snake antivenin natural products in West Africa. ChemMedChem. 2021;16(24):3635-3648. doi:10.1002/cmdc.202100478.
34. Yusuf A, Bugaje A, Sadiq M, Salihu M, Adamu H, Abdulrahman M. Inhibitory potential of phytochemicals from *Vernonia glaberrima* leaves against snake venom toxins: computational and experimental validation. Toxicon. 2024; 247:107838. doi: 10.1016/j.toxicon.2024.107838.
35. Bolon I, Durso AM, Botero Mesa S, Ray N, Alcoba G, Chappuis F, Ruiz de Castañeda R. Identifying the snake: First scoping review on practices of communities and healthcare providers confronted with snakebite across the world. PLoS one. 2020 Mar 5;15(3): e0229989.